Hindawi Publishing Corporation
Mathematical Problems in Engineering
Volume 2011, Article ID 567489, 18 pages
doi:10.1155/2011/567489

Research Article

Dynamic Analysis of Cracked Octagonal Quasicrystals

Wu Li[1,2] and Tian You Fan[2]

[1] *Institute of Applied Mathematics, Xuchang University, Xuchang 461000, China*
[2] *Department of Mathematics, School of Science, Beijing Institute of Technology, Beijing 100081, China*

Correspondence should be addressed to Wu Li, liwu823210@126.com

Received 29 March 2011; Accepted 5 July 2011

Academic Editor: Mehrdad Massoudi

We focus on the dynamic fracture problem of octagonal quasicrystals by applying a rectangular sample with a Griffith crack which is often used in classical elastic media based on the method of finite difference. This paper mainly is to investigate the variation of phonon, phason fields, and stress singularity around the crack tip including the stress intensity factor. In addition, the moving boundary due to the crack propagation has also been treated by introducing an additional condition for determining solution. The influence of wave propagation and diffusion in the dynamic process is also discussed in detail. Through comparing the results of octagonal quasicrystals with the results of crystal, this paper proclaims the influence of phonon-phason coupling in dynamic fracture problem of octagonal quasicrystals which should not be neglected.

1. Introduction

Quasicrystals are a form of solids different from both crystals and glassy solids, which possess quasiperiodic long-range translational symmetry and noncrystallographic rotational symmetry [1]. Due to the quasiperiodicity, quasicrystals have a special type of elastic degrees of freedom, termed as phason degrees of freedom apart from phonon degrees which exist too for crystals. Under given load conditions, they are giving rise to two displacement fields $\mathbf{u}(\mathbf{r},t)$ for phonon field and $\mathbf{w}(\mathbf{r},t)$ for phason field, which also yield the elastic strain tensors ε_{ij} and w_{ij}, respectively [2–4],

$$\varepsilon_{ij} \equiv \frac{1}{2}\left(\frac{\partial u_i}{\partial x_j} + \frac{\partial u_j}{\partial x_i}\right), \qquad w_{ij} \equiv \frac{\partial w_i}{\partial x_j} \quad (w_{ij} \neq w_{ji}). \tag{1.1}$$

In linear elasticity the stress tensors are related to the strain tensors obtained by [2]

$$\sigma_{ij} = C_{ijkl}\varepsilon_{kl} + R_{ijkl}w_{kl}, \qquad H_{ij} = R_{klij}\varepsilon_{kl} + K_{ijkl}w_{kl}, \tag{1.2}$$

where u_i, w_i are phonon and phason displacements, σ_{ij} and ε_{ij} phonon stresses and strains, H_{ij} and w_{ij} phason stresses and strains, C_{ijkl}, K_{ijkl}, and R_{ijkl} the phonon, phason, phonon-phason coupling elastic constants, respectively. But for the elasto-/hydro-dynamics, there are different theoretical points of view, for example, those being put forward by Bak [5, 6] and by Lubensky et al [7]. Here we adopt the viewpoint raised by Fan [2]:

$$\begin{aligned} \rho\frac{\partial^2 u_i}{\partial t^2} &= \frac{\partial \sigma_{ij}}{\partial x_j}, \\ \frac{1}{\Gamma_w}\frac{\partial w_i}{\partial t} &= \frac{\partial H_{ij}}{\partial x_j}, \end{aligned} \tag{1.3}$$

in which $\Gamma_w = 1/\kappa$ denotes the kinetic coefficient of phason field.

For this subject, Zhu and Fan and Wang et al. have used the icosahedral Al-Pd-Mn quasicrystal and the decagonal Al-Ni-Co quasicrystal to simulate dynamic behaviour of quasicrystals [8, 9]. However, little attention has been devoted to the octagonal quasicrystals which occupy a very important position in this solids. Of course, there are many theoretical and experimental results reported up to now [10–33]. Their results could be better convinced if they have considered the dynamic behaviour of octagonal quasicrystals.

In the following sections, we will reveal the dynamic fracture behaviour of octagonal quasicrystals by introducing a rectangular sample with a Griffith crack based on the method of finite difference. In the end, we explain physical significance of the results obtained in the paper. Of course, further studies of the quasicrystals should be consummated by the future results. It is hoped that the dynamics question of quasicrystals will be observed by experiments.

2. Basic Formulas and Simplified Model

We focus on the solution for the plane elasticity of the octagonal quasicrystals that is, the atom arrangement along the z-direction is periodic and along the $x - y$ plane is quasiperiodic. For the octagonal quasicrystals, we have the elastic constants matrix [**CKR**]:

$$[\mathbf{CKR}] = \begin{bmatrix} L+2M & L & 0 & 0 & R & R & 0 & 0 \\ L & L+2M & 0 & 0 & -R & -R & 0 & 0 \\ 0 & 0 & M & M & 0 & 0 & -R & R \\ 0 & 0 & M & M & 0 & 0 & -R & R \\ R & -R & 0 & 0 & K_1 & K_2 & 0 & 0 \\ R & -R & 0 & 0 & K_2 & K_1 & 0 & 0 \\ 0 & 0 & -R & -R & 0 & 0 & K_1+K_2+K_3 & K_3 \\ 0 & 0 & R & R & 0 & 0 & K_3 & K_1+K_2+K_3 \end{bmatrix}. \tag{2.1}$$

In this case, the stress-strain relations are reduced to (2.2) from (2.1),

$$\begin{aligned}
\sigma_{xx} &= L(\varepsilon_{xx}+\varepsilon_{yy})+2M\varepsilon_{xx}+R(w_{xx}+w_{yy}),\\
\sigma_{yy} &= L(\varepsilon_{xx}+\varepsilon_{yy})+2M\varepsilon_{yy}-R(w_{xx}+w_{yy}),\\
\sigma_{xy} &= \sigma_{yx}=2M\varepsilon_{xy}+R(w_{yx}-w_{xy}),\\
H_{xx} &= K_1w_{xx}+K_2w_{yy}+R(\varepsilon_{xx}-\varepsilon_{yy}),\\
H_{yy} &= K_1w_{yy}+K_2w_{xx}+R(\varepsilon_{xx}-\varepsilon_{yy}),\\
H_{xy} &= (K_1+K_2+K_3)w_{xy}+K_3w_{yx}-2R\varepsilon_{xy},\\
H_{yx} &= (K_1+K_2+K_3)w_{yx}+K_3w_{xy}+2R\varepsilon_{xy},
\end{aligned} \tag{2.2}$$

where $L = C_{12}$, $M = (C_{11} - C_{12})/2$ are the phonon elastic constants, K_1, K_2, and K_3 are the phason elastic constants, and R is phonon-phason coupling elastic constant.

Substituting (2.2) into (1.3), we obtain the equations of motion of octagonal quasicrystals given by displacement components as follows:

$$\begin{aligned}
\frac{\partial^2 u_x}{\partial t^2} &= c_1^2\frac{\partial^2 u_x}{\partial x^2}+\left(c_1^2-c_2^2\right)\frac{\partial^2 u_y}{\partial x\partial y}+c_2^2\frac{\partial^2 u_x}{\partial y^2}+c_3^2\left(\frac{\partial^2 w_x}{\partial x^2}+2\frac{\partial^2 w_y}{\partial x\partial y}-\frac{\partial^2 w_x}{\partial y^2}\right),\\
\frac{\partial^2 u_y}{\partial t^2} &= c_2^2\frac{\partial^2 u_y}{\partial x^2}+\left(c_1^2-c_2^2\right)\frac{\partial^2 u_x}{\partial x\partial y}+c_1^2\frac{\partial^2 u_y}{\partial y^2}+c_3^2\left(\frac{\partial^2 w_y}{\partial x^2}-2\frac{\partial^2 w_x}{\partial x\partial y}-\frac{\partial^2 w_y}{\partial y^2}\right),\\
\frac{\partial w_x}{\partial t} &= d_1^2\frac{\partial^2 w_x}{\partial x^2}+d_2^2\frac{\partial^2 w_x}{\partial y^2}+\left(d_2^2-d_1^2\right)\frac{\partial^2 w_y}{\partial x\partial y}+d_3^2\left(\frac{\partial^2 u_x}{\partial x^2}-2\frac{\partial^2 u_y}{\partial x\partial y}-\frac{\partial^2 u_x}{\partial y^2}\right),\\
\frac{\partial w_y}{\partial t} &= d_1^2\frac{\partial^2 w_y}{\partial x^2}+d_2^2\frac{\partial^2 w_y}{\partial y^2}+\left(d_2^2-d_1^2\right)\frac{\partial^2 w_x}{\partial x\partial y}+d_3^2\left(\frac{\partial^2 u_y}{\partial x^2}+2\frac{\partial^2 u_x}{\partial x\partial y}-\frac{\partial^2 u_y}{\partial y^2}\right),
\end{aligned} \tag{2.3}$$

in which

$$\begin{aligned}
&c_1=\sqrt{\frac{L+2M}{\rho}}, \qquad c_2=\sqrt{\frac{M}{\rho}}, \qquad c_3=\sqrt{\frac{R}{\rho}},\\
&d_1=\sqrt{\frac{K_1}{\kappa}}, \qquad d_2=\sqrt{\frac{K_1+K_2+K_3}{\kappa}}, \qquad d_3=\sqrt{\frac{R}{\kappa}},
\end{aligned} \tag{2.4}$$

note that constants c_1, c_2, and c_3 have the meaning of elastic wave speeds, while d_1^2, d_2^2, and d_3^2 do not represent wave speed; they are diffusive coefficients.

To ensure the uniform configuration along the periodic direction physically and geometrically, we consider such model that a rectangular octagonal quasicrystal containing a Griffith crack in the center is subjected a dynamic tensile stress on both upper and lower boundaries. Assume that the Griffith crack penetrates through the solid along the periodic direction. As shown in Figure 1(a), the size of the specimen is that ED equals to $2L$ and EF

Table 1: The related parameters used in numerical computation [24, 26, 28] (unit: 10^{12} dyn/cm^2).

C_{11}	C_{12}	K_1	K_2	K_3	κ	ρ
2.3430	0.5741	1.2000	0.2400	0.1200	$1/4.8 \times 10^{10}$ g/cm$^3 \cdot \mu$s	54.186×10^{-3} g/cm^3

equals to $2H$, and a is the length of the crack, which is constant, and $p(t)$ is the dynamic load, which varies with time. This represents the condition of the initiation of crack growth. As shown in Figure 1(b), the conditions are almost the same to that in Figure 1(a) except that the length of the crack $a(t)$ is a function of time instead of constant and the dynamic load $p(t)$ becomes constant.

As shown in Figures 1(a) and 1(b), only the upper right quarter needs to consider due to the symmetry. Referring to the upper right part and considering a fix grips case, the following boundary conditions should be satisfied:

$$\begin{aligned}
&u_x = 0, \quad \sigma_{yx} = 0, \quad w_x = 0, \quad H_{yx} = 0 \quad \text{on } x = 0 \text{ for } 0 \le y \le H,\\
&\sigma_{xx} = 0, \quad \sigma_{yx} = 0, \quad H_{xx} = 0, \quad H_{yx} = 0 \quad \text{on } x = L \text{ for } 0 \le y \le H,\\
&\sigma_{yy} = p(t), \quad \sigma_{xy} = 0, \quad H_{yy} = 0, \quad H_{xy} = 0 \quad \text{on } y = H \text{ for } 0 \le x \le L,\\
&\sigma_{yy} = 0, \quad \sigma_{xy} = 0, \quad H_{yy} = 0, \quad H_{xy} = 0 \quad \text{on } y = 0 \text{ for } 0 \le x \le a(t),\\
&u_y = 0, \quad \sigma_{xy} = 0, \quad w_y = 0, \quad H_{xy} = 0 \quad \text{on } y = 0 \text{ for } a(t) \le x \le L,
\end{aligned} \tag{2.5}$$

in which $p(t)$ is the dynamic load.

In addition, the initial conditions including the initial displacement and velocity are equal to zeroes:

$$\begin{aligned}
&u_x(x,y,t)|_{t=0} = 0, \qquad u_y(x,y,t)|_{t=0} = 0,\\
&w_x(x,y,t)|_{t=0} = 0, \qquad w_y(x,y,t)|_{t=0} = 0,\\
&\frac{\partial u_x}{\partial t}(x,y,t)|_{t=0} = 0, \qquad \frac{\partial u_y}{\partial t}(x,y,t)|_{t=0} = 0.
\end{aligned} \tag{2.6}$$

In the following section, we let the related parameters $2H = 40$ mm and $2L = 20$ mm, the initial length $a_0 = 2.4$ mm of the crack, and elastic constants can be found in Table 1.

3. Demonstrations of the Finite Difference Method and the Results

The final governing equation (2.3) along with boundary conditions equation (2.5) and initial conditions equation (2.6) are very complicated, analytic solution for the boundary-initial value problem is not available at present, which has to be solved by numerical method. Here we extend the method of finite difference of Shmuely and Alterman [22] scheme for analyzing crack problem for conventional engineering materials to quasicrystalline materials. A grid is imposed on the upper right of the specimen shown in Figure 2, the grid is extended beyond the half step.

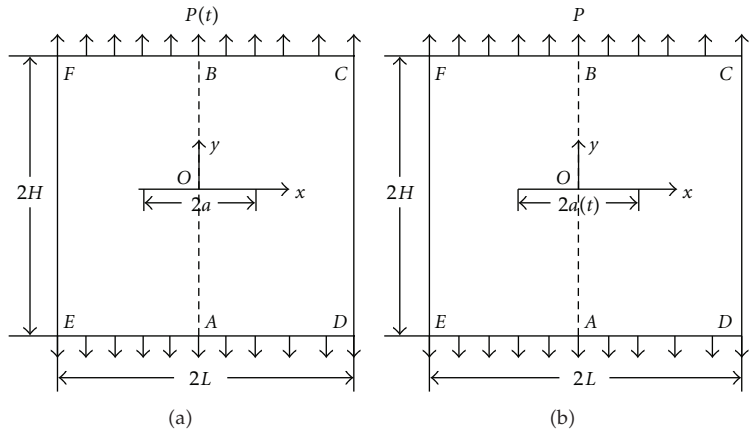

Figure 1: Sample of cracked quasicrystal under tension: (a) Crack stable with a dynamic load, (b) Crack fast propagation with a constant load.

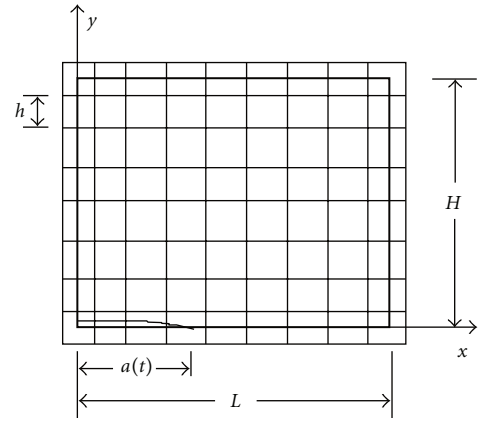

Figure 2: Finite difference scheme quarter specimen.

Taking the finite difference scheme proposed by [22], (2.3) and the conditions equations (2.5) and (2.6) can be reduced to certain difference equations to solve. The details on numerical computation are listed in the Appendix. To check the validity of the model and the accuracy of the algorithm, at first we give a numerical example for phason displacement. Figure 3 depicts displacement component of phason field w_x versus time. According to the present model phasons represent diffusion, the computational results indicate this is true, and the component w_x is identical to the fundamental solution of pure diffusion in mathematical physics, that is,

$$w \sim \frac{1}{\sqrt{t-t_0}} e^{-(x-x_0)^2/\Gamma_w(t-t_0)}, \tag{3.1}$$

where t is the time t_0 is a special value of t, x is a distance, and x_0 is a special value of x. Though there is small fluctuation around the fundamental solution due to phonon-phason coupling, this checking confirms that the model is reasonable and the finite difference method

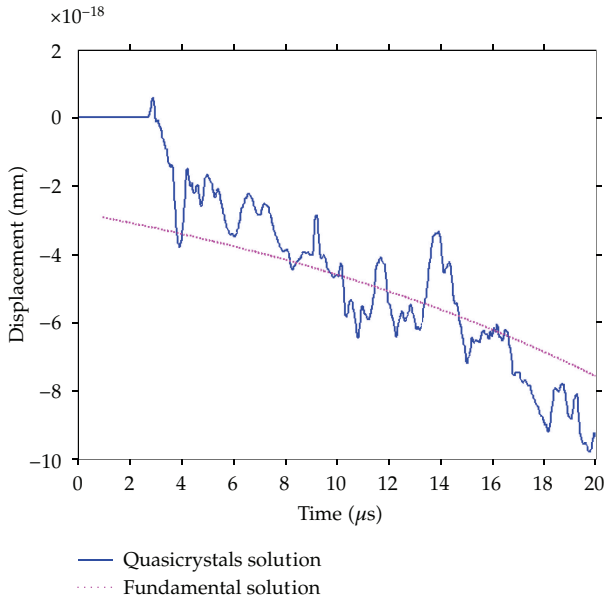

Figure 3: Displacement component of phason field w_x versus time and comparison with the fundamental solution of pure diffusion equation in mathematical physics.

and its computer implementation are effective and of high accuracy. In addition the phonons present the character of wave propagation this is natural and easily understood, and need not to give additional discussion and graphic illustration.

In the "phase" of dynamic initiation of crack growth, the specimen with stationary crack assuming $a(t)$ = constant is subjected to a rapidly varying load $p(t) = pf(t)$, where $f(t)$ is taken as the Heaviside function. The stresses at the crack tip present singularity of order $r^{-1/2}$, where r denotes the distance from the crack tip, so that we can obtain the dynamic stress intensity factor for phonon stress field such as

$$K_I(t) = \lim_{x \to a^+} \sqrt{2\pi(x-a)}\sigma_{yy}(x,0,t) \tag{3.2}$$

and the normalized dynamics stress intensity factor; that is, $K_I(t)/\sqrt{\pi a}p$ ($\sqrt{\pi a}p$ denotes the static stress intensity factor of a Griffith crack) versus time is depicted in Figure 4.

In Figure 4, there are two curves in the figure: one represents quasicrystal, that is, $R/M = 0.01$, and the other describes periodic crystals corresponding to $R/M = 0$. Because of the phonon-phason coupling effect, the mechanical properties of the quasicrystals are obviously different from the classical crystals. But the phonon wave propagation plays dominating role in dynamics of quasicrystals.

The follows are the cases that the specimen with a stationary crack are subjected to two most common types of pulse dynamic load. The pulses possess different period T_0, respectively.

From Figure 5, it can be easily concluded that S.I.F. is influenced greatly by the shape of the load of the pulse imposed. Also it is interesting that there is a time of lag between the variables and the load getting extremum. The reason for that is the influence of stress wave

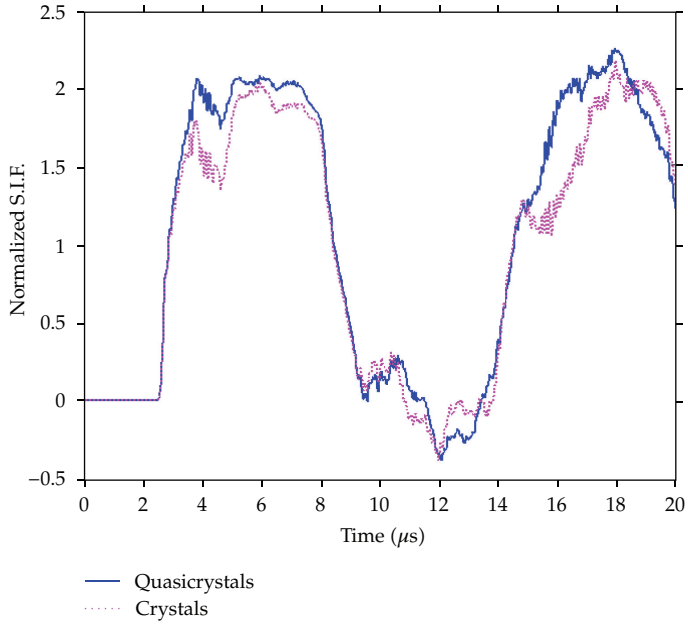

Figure 4: Normalized S.I.F. for phonon stress field versus time.

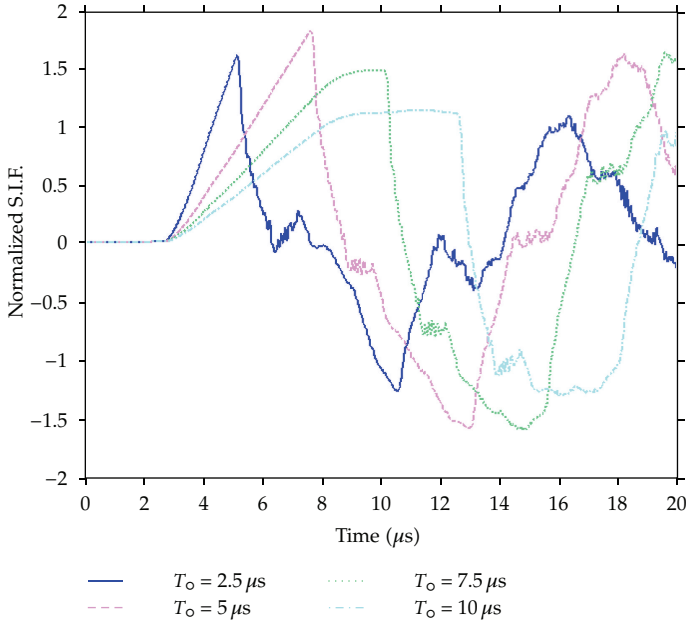

Figure 5: Normalized S.I.F. versus time for different wave length of zigzag pulse dynamic loads.

propagation as well as the effect of refraction and reflection. It is obviously seen that the shape of these sets of waves in the initial is like sawtooth. there will be of a bit fluctuations in the process when the wave reaches the second peak value. From the above analysis it can be concluded that the curve of S.I.F. is influenced greatly by the shape of the load of the pulse imposed, and the shapes of both are similar.

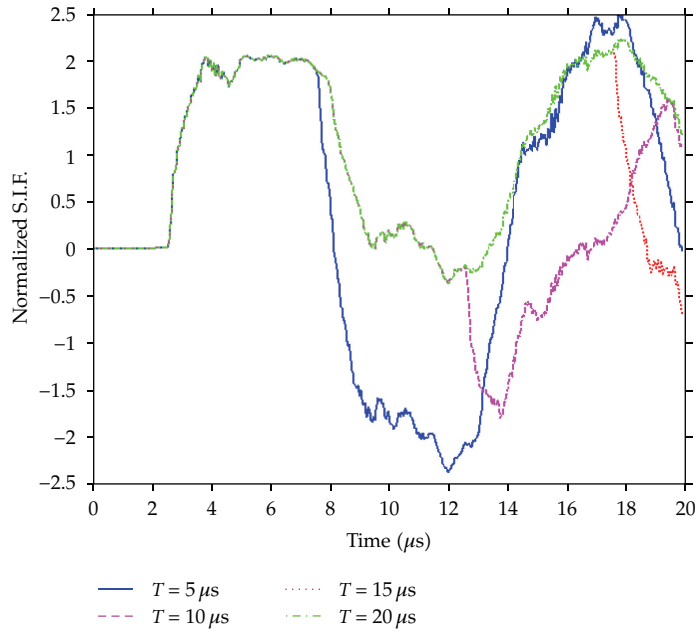

Figure 6: Normalized S.I.F. versus time for different wave length of rectangular pulse dynamic loads.

From Figure 6, we conclude that the curved line of S.I.F. has relationships with the energy of the relative load. The larger the time of the pulse continues, the more mildly the S.I.F. varies also in the same conditions S.I.F. is larger on average in the long run.

Now we focus on the discussion for the "phase" of fast crack propagation. To explore the inertia effect caused by the fast crack propagation, the specimen are designed under the action of constant load $p(t) = p$ rather than time-varying load, but the crack grows with high speed. The problem for fast crack propagation is a nonlinear problem, because one part of the boundaries' crack is of unknown length beforehand. For this moving boundary problem, we must give additional condition for determining solution. That is, we must give a criterion checking crack propagation or crack arrest at the growing crack tip. This criterion can be imposed in different ways, for example, the critical stress criterion or critical energy criterion. The stress criterion is used in this paper: $\sigma_{yy} < \sigma_c$ represents crack arrest, $\sigma_{yy} = \sigma_c$ represents critical state, and $\sigma_{yy} > \sigma_c$ represents crack propagation. Here $\sigma_c = 450$ Mpa is adopted as this criterion. The detailed introduction is cited from [2].

The crack velocity for quasicrystals and periodic crystals is constructed in Figure 7, from which, we can see that the velocity in quasicrystals is lower than that of the periodic crystals. The simulation reveals the dominating role of highly coordinate atomic environment as structure-intrinsic obstacles for crack propagation. For explaining this phenomenon we can explain a specific crack propagation mechanism: because the phonon-phason coupling makes the quasicrystals different from periodic crystals, the crack tip propagation velocity maybe hindered by phonon-phason coupling effect. Though the term seems like that introduced by [32], the meaning of them is different.

Next we will explore the velocity under different loads in quasicrystal. The above described procedure was conducted, keeping the same geometry and material constants. With various loads, the relation between velocity and crack growth is depicted in Figure 8. It

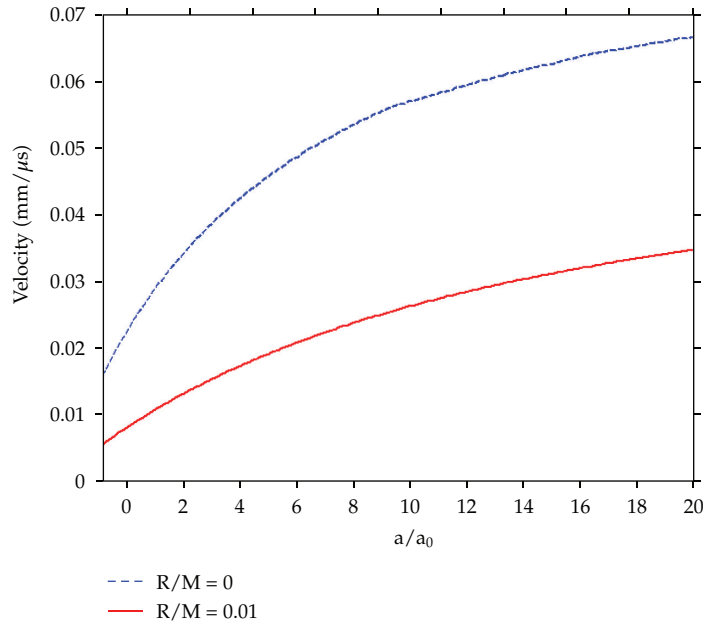

Figure 7: The crack velocity versus normalized crack size with different coupling constants with $p = 1$ Mpa.

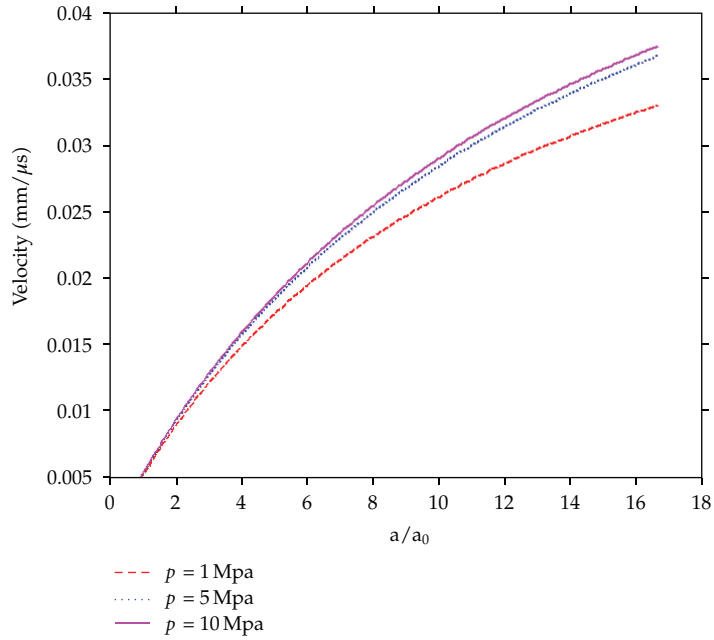

Figure 8: Variation of crack velocity versus crack growth size for different load levels.

is understandable, while the load is increasing, the time to reach the stress criterion is short; so that the velocity becomes fast.

For the profile of growing crack shown in Figure 9, presents roughness when load level is growing, but there is no experimental observation for fast crack propagation though Ebert et al. had made some observation by scanning tunneling microscopy for quasistatic

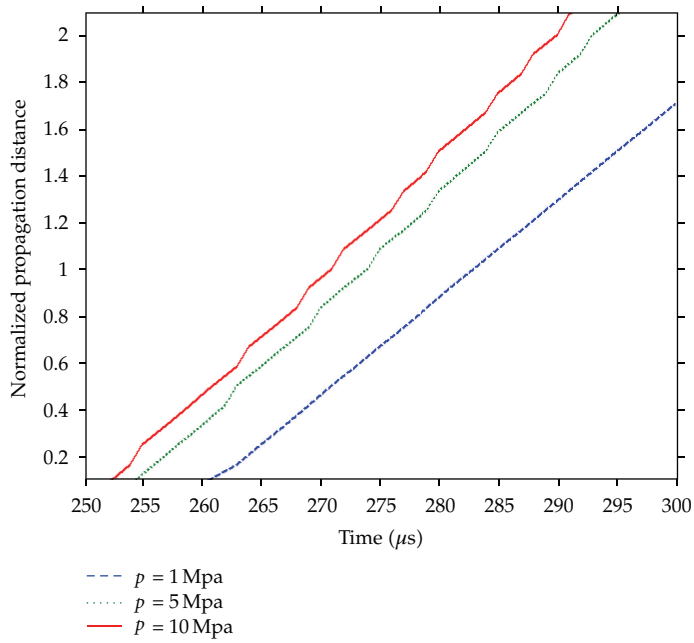

Figure 9: Normalized crack growth size $(a - a_0)/a_0$ of crack tip versus time for different load levels.

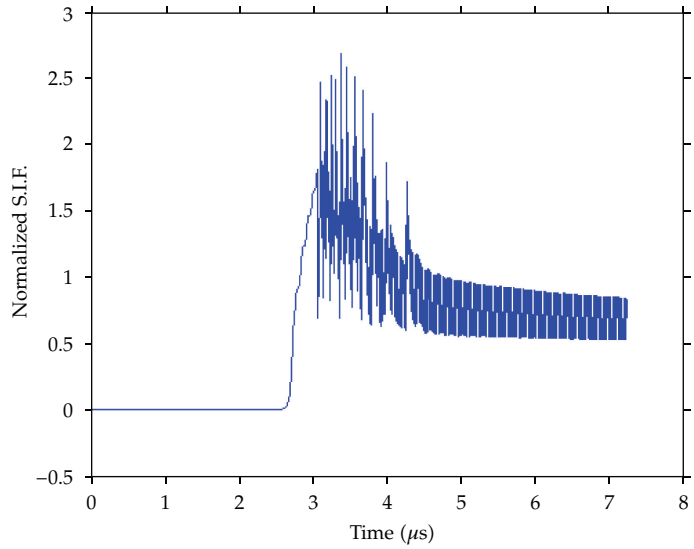

Figure 10: Normalized S.I.F. for quasicrystal in the criterion σ_c = 450 Mpa.

crack growth [33]. Because the fast propagation and quasistatic crack growth belong to two different regimes, the comparison cannot be done.

In Figure 10, we can see that the fluctuation of normalized S.I.F. is very large when the criterion σ_c = 450 Mpa, that is, because the surface of the crack is not flat.

4. Conclusion and Discussion

The dynamic fracture process of octagonal quasicrystals occupies an important position in dynamic response of quasicrystals. Of course, many analytic solutions which are related to the static mechanics of octagonal quasicrystals have been obtained. But obtaining the analytic solution of dynamic fracture process of octagonal quasicrystals is very difficult. In this paper, we simulate dynamic fracture process of octagonal quasicrystals. Because the analytic solution about it is not available, we develop the finite difference procedure based on argument of Bak as well as argument of Lubensky et al., which can also be seen as a collaborating model of wave propagation and motion of diffusion. Numerical results reveal the validity of wave propagation behavior of phonon field and behavior of motion of diffusion of phason field; the interaction between phonons and phasons is also recorded. The dominant physical quantities (i.e., stress intensity factors) have been discussed in detail. The formulism is applied to analysis of dynamic initiation of crack growth and crack fast propagation for two-dimensional octagonal quasicrystals of point group 8 mm the displacement and stress fields around the tip of stationary and propagating cracks are revealed. The results show that the phonon-phason coupling plays an important role in dynamic fracture behaviour of octagonal quasicrystals, which is different from crystals.

Appendix

The Details of Finite Difference Scheme

Here we extend the method of finite difference of Shmuely and Alterman scheme for analyzing crack problem for conventional engineering materials to quasicrystalline materials. A grid is imposed on the upper right of the specimen shown in Figure 2. For convenience, the mesh size h is taken to be the same in both x and y directions. The grid is extended beyond the half step by adding four special grid lines $x = -h/2$, $x = L + h/2$, $y = -h/2$, and $y = H + h/2$ which form the grid boundaries. Denoting the time step by τ and using central difference approximations, the finite difference formulations for the above text are

$$\begin{aligned}
u_x(x,y,t+\tau) &= 2u_x(x,y,t) - u_x(x,y,t-\tau) \\
&\quad + \left(\frac{\tau}{h}c_1\right)^2 \left[u_x(x+h,y,t) - 2u_x(x,y,t) + u_x(x-h,y,t)\right] \\
&\quad + \left(\frac{\tau}{h}\right)^2 \left(c_1^2 - c_2^2\right) \left[u_y(x+h,y+h,t) - u_y(x+h,y-h,t)\right. \\
&\qquad \left. - u_y(x-h,y+h,t) + u_y(x-h,y-h,t)\right] \\
&\quad + \left(\frac{\tau}{h}c_2\right)^2 \left[u_x(x,y+h,t) - 2u_x(x,y,t) + u_x(x,y-h,t)\right] \\
&\quad + \left(\frac{\tau}{h}c_3\right)^2 \left[w_x(x+h,y,t) - 2w_x(x,y,t) + w_x(x-h,y,t)\right]
\end{aligned}$$

$$+2\left(\frac{\tau}{h}\right)^2 c_3^2\left[w_y(x+h,y+h,t)-w_y(x+h,y-h,t)-w_y(x-h,y+h,t)\right.$$
$$\left.+w_y(x-h,y-h,t)\right]$$
$$-\left(\frac{\tau}{h}c_3\right)^2\left[w_x(x,y+h,t)-2w_x(x,y,t)+w_x(x,y-h,t)\right], \tag{A.1a}$$

$$u_y(x,y,t+\tau)=2u_y(x,y,t)-u_y(x,y,t-\tau)+\left(\frac{\tau}{h}c_2\right)^2$$
$$\times\left[u_y(x+h,y,t)-2u_y(x,y,t)+u_y(x-h,y,t)\right]+\left(\frac{\tau}{2h}\right)^2\left(c_1^2-c_2^2\right)$$
$$\times\left[u_x(x+h,y+h,t)-u_x(x+h,y-h,t)-u_x(x-h,y+h,t)+u_x(x-h,y-h,t)\right]$$
$$+\left(\frac{\tau}{h}c_1\right)^2\left[u_y(x,y+h,t)-2u_y(x,y,t)+u_y(x,y-h,t)\right]+\left(\frac{\tau}{h}c_3\right)^2$$
$$\times\left[w_y(x+h,y,t)-2w_y(x,y,t)+w_y(x-h,y,t)\right]-2\left(\frac{\tau}{2h}\right)^2 c_3^2$$
$$\times\left[w_x(x+h,y+h,t)-w_x(x+h,y-h,t)-w_x(x-h,y+h,t)\right.$$
$$\left.+w_x(x-h,y-h,t)\right]-\left(\frac{\tau}{h}c_3\right)^2$$
$$\times\left[w_y(x,y+h,t)-2w_y(x,y,t)+w_y(x,y-h,t)\right], \tag{A.1b}$$

$$w_x(x,y,t+\tau)=w_x(x,y,t)-d_3^2\frac{\tau}{h^2}\left[u_x(x+h,y,t)-2u_x(x,y,t)+u_x(x-h,y,t)\right]$$
$$+d_1^2\frac{\tau}{h^2}\left[w_x(x+h,y,t)-2w_x(x,y,t)+w_x(x-h,y,t)\right]$$
$$+d_2^2\frac{\tau}{h^2}\left[w_x(x,y+h,t)-2w_x(x,y,t)+w_x(x,y-h,t)\right]$$
$$-\frac{1}{2}d_3^2\frac{\tau}{h^2}\left[u_y(x+h,y+h,t)-u_y(x+h,y-h,t)-u_y(x-h,y+h,t)\right.$$
$$\left.+u_y(x-h,y-h,t)\right]+\frac{(d_2^2-d_1^2)\tau}{(2h)^2}$$
$$\times\left[w_y(x+h,y+h,t)-w_y(x+h,y-h,t)-w_y(x-h,y+h,t)\right.$$
$$\left.+w_y(x-h,y-h,t)\right]$$
$$-d_3^2\frac{\tau}{h^2}\left[u_x(x,y+h,t)-2u_x(x,y,t)+u_x(x,y-h,t)\right], \tag{A.1c}$$

$$
\begin{aligned}
w_y(x,y,t+\tau) = {} & w_y(x,y,t) - d_3^2\frac{\tau}{h^2}\left[u_y(x+h,y,t) - 2u_y(x,y,t) + u_y(x-h,y,t)\right] \\
& + d_1^2\frac{\tau}{h^2}\left[w_y(x+h,y,t) - 2w_y(x,y,t) + w_y(x-h,y,t)\right] \\
& + d_2^2\frac{\tau}{h^2}\left[w_y(x,y+h,t) - 2w_y(x,y,t) + w_y(x,y-h,t)\right] \\
& - \frac{1}{2}d_3^2\frac{\tau}{h^2}\left[u_x(x+h,y+h,t) - u_x(x+h,y-h,t) - u_x(x-h,y+h,t)\right. \\
& \qquad \left. + u_x(x-h,y-h,t)\right] + \frac{(d_2^2 - d_1^2)\tau}{(2h)^2} \\
& \times \left[w_x(x+h,y+h,t) - w_x(x+h,y-h,t) - w_x(x-h,y+h,t)\right. \\
& \qquad \left. + w_x(x-h,y-h,t)\right] \\
& - d_3^2\frac{\tau}{h^2}\left[u_y(x,y+h,t) - 2u_y(x,y,t) + u_y(x,y-h,t)\right].
\end{aligned}
\tag{A.1d}
$$

The displacements at mesh points located at the special lines are determined by satisfying the boundary conditions; we obtain, respectively, for points on the grid lines $x = -h/2$ and $x = L + h/2$

$$
\begin{aligned}
u_x\left(\begin{matrix} -\frac{h}{2} \\ L+\frac{h}{2} \end{matrix}, y, t\right) = {} & u_x\left(\begin{matrix} \frac{h}{2} \\ L-\frac{h}{2} \end{matrix}, y, t\right) \pm \frac{1}{2}\frac{d_1^2(c_1^2 - 2c_2^2) + c_3^2 d_3^2}{c_1^2 d_1^2 - c_3^2 d_3^2} \\
& \times \left[u_y\left(\begin{matrix} \frac{h}{2} \\ L-\frac{h}{2} \end{matrix}, y+h, t\right) - u_y\left(\begin{matrix} \frac{h}{2} \\ L-\frac{h}{2} \end{matrix}, y-h, t\right)\right] \\
& \mp \frac{1}{2}\frac{c_3^2(d_2^2 - 2d_1^2 - d_4^2)}{c_1^2 d_1^2 - c_3^2 d_3^2} \\
& \times \left[w_y\left(\begin{matrix} \frac{h}{2} \\ L-\frac{h}{2} \end{matrix}, y+h, t\right) - w_y\left(\begin{matrix} \frac{h}{2} \\ L-\frac{h}{2} \end{matrix}, y-h, t\right)\right],
\end{aligned}
\tag{A.2a}
$$

$$
\begin{aligned}
w_x\left(\begin{matrix} -\frac{h}{2} \\ L+\frac{h}{2} \end{matrix}, y, t\right) = {} & w_x\left(\begin{matrix} \frac{h}{2} \\ L-\frac{h}{2} \end{matrix}, y, t\right) \pm \frac{d_3^2(c_2^2 - c_1^2)}{c_1^2 d_1^2 - c_3^2 d_3^2} \\
& \times \left[u_y\left(\begin{matrix} \frac{h}{2} \\ L-\frac{h}{2} \end{matrix}, y+h, t\right) - u_y\left(\begin{matrix} \frac{h}{2} \\ L-\frac{h}{2} \end{matrix}, y-h, t\right)\right]
\end{aligned}
$$

$$\pm\frac{1}{2}\frac{c_1^2\left(d_2^2-d_1^2-d_4^2\right)-c_3^2d_3^2}{c_1^2d_1^2-c_3^2d_3^2}\times\left[w_y\left(\begin{matrix}\frac{h}{2}\\ L-\frac{h}{2}\end{matrix},y+h,t\right)-w_y\left(\begin{matrix}\frac{h}{2}\\ L-\frac{h}{2}\end{matrix},y-h,t\right)\right], \tag{A.2b}$$

$$u_y\left(\begin{matrix}-\frac{h}{2}\\ L+\frac{h}{2}\end{matrix},y,t\right)=u_y\left(\begin{matrix}\frac{h}{2}\\ L-\frac{h}{2}\end{matrix},y,t\right)\pm\frac{1}{2}\left[u_x\left(\begin{matrix}\frac{h}{2}\\ L-\frac{h}{2}\end{matrix},y+h,t\right)-u_x\left(\begin{matrix}\frac{h}{2}\\ L-\frac{h}{2}\end{matrix},y-h,t\right)\right]\mp\frac{1}{2}\frac{c_3^2\left(d_2^2+d_4^2\right)}{c_2^2d_2^2-c_3^2d_3^2}\left[w_x\left(\begin{matrix}\frac{h}{2}\\ L-\frac{h}{2}\end{matrix},y+h,t\right)-w_x\left(\begin{matrix}\frac{h}{2}\\ L-\frac{h}{2}\end{matrix},y-h,t\right)\right], \tag{A.2c}$$

$$w_y\left(\begin{matrix}-\frac{h}{2}\\ L+\frac{h}{2}\end{matrix},y,t\right)=w_y\left(\begin{matrix}\frac{h}{2}\\ L-\frac{h}{2}\end{matrix},y,t\right)\pm\frac{1}{2}\frac{c_3^2d_3^2+c_2^2d_4^2}{c_2^2d_2^2-c_3^2d_3^2}\times\left[w_x\left(\begin{matrix}\frac{h}{2}\\ L-\frac{h}{2}\end{matrix},y+h,t\right)-w_x\left(\begin{matrix}\frac{h}{2}\\ L-\frac{h}{2}\end{matrix},y-h,t\right)\right], \tag{A.2d}$$

where (A.2a) and (A.2b) related to $x=-h/2$ are not valid. From the first condition of (2.5), at $x=0$, $u_x=0$ and $w_x=0$. To satisfy the condition the displacements u_x and w_x at $x=-h/2$ are approximated by

$$u_x\left(x,-\frac{h}{2},t\right)=-u_x\left(x,\frac{h}{2},t\right),\qquad w_x\left(x,-\frac{h}{2},t\right)=-w_x\left(x,\frac{h}{2},t\right). \tag{A.3}$$

On the grid line $y=-h/2$ and $y=H+h/2$, we obtain

$$u_x\left(\begin{matrix}x,\\ L+\frac{h}{2}\end{matrix}\begin{matrix}-\frac{h}{2}\\ \end{matrix},t\right)=u_x\left(\begin{matrix}x,\\ L-\frac{h}{2}\end{matrix}\begin{matrix}-\frac{h}{2}\\ \end{matrix},t\right)$$

$$\pm\frac{1}{2}\left[u_y\left(\begin{matrix}x+h,\\ L-\dfrac{h}{2}\end{matrix}\begin{matrix}\dfrac{h}{2}\\ ,t\end{matrix}\right)-u_y\left(\begin{matrix}x-h,\\ L-\dfrac{h}{2}\end{matrix}\begin{matrix}\dfrac{h}{2}\\ ,t\end{matrix}\right)\right]$$

$$\pm\frac{1}{2}\frac{c_3^2\left(d_1^2-d_3^2\right)}{c_2^2d_1^2-c_3^2d_2^2}\left[w_y\left(\begin{matrix}x+h,\\ L-\dfrac{h}{2}\end{matrix}\begin{matrix}\dfrac{h}{2}\\ ,t\end{matrix}\right)-w_y\left(\begin{matrix}x-h,\\ L-\dfrac{h}{2}\end{matrix}\begin{matrix}\dfrac{h}{2}\\ ,t\end{matrix}\right)\right], \tag{A.4a}$$

$$w_x\left(\begin{matrix}x,\\ L+\dfrac{h}{2}\end{matrix}\begin{matrix}-\dfrac{h}{2}\\ ,t\end{matrix}\right)=w_x\left(\begin{matrix}x,\\ L-\dfrac{h}{2}\end{matrix}\begin{matrix}-\dfrac{h}{2}\\ ,t\end{matrix}\right)$$

$$\pm\frac{1}{2}\frac{c_3^2d_2^2-c_2^2d_3^2}{c_2^2d_1^2-c_3^2d_2^2}\left[w_y\left(\begin{matrix}x+h,\\ L-\dfrac{h}{2}\end{matrix}\begin{matrix}\dfrac{h}{2}\\ ,t\end{matrix}\right)-w_y\left(\begin{matrix}x-h,\\ L-\dfrac{h}{2}\end{matrix}\begin{matrix}\dfrac{h}{2}\\ ,t\end{matrix}\right)\right], \tag{A.4b}$$

$$u_y\left(\begin{matrix}x,\\ L+\dfrac{h}{2}\end{matrix}\begin{matrix}-\dfrac{h}{2}\\ ,t\end{matrix}\right)=u_y\left(\begin{matrix}x,\\ L-\dfrac{h}{2}\end{matrix}\begin{matrix}\dfrac{h}{2}\\ ,t\end{matrix}\right)\pm\frac{1}{2}\frac{c_3^2d_2^2+d_1^2\left(c_1^2-2c_2^2\right)}{c_1^2d_1^2-c_3^2d_2^2}$$

$$\times\left[u_x\left(\begin{matrix}x+h,\\ L-\dfrac{h}{2}\end{matrix}\begin{matrix}\dfrac{h}{2}\\ ,t\end{matrix}\right)-u_x\left(\begin{matrix}x-h,\\ L-\dfrac{h}{2}\end{matrix}\begin{matrix}\dfrac{h}{2}\\ ,t\end{matrix}\right)\right]$$

$$\pm\frac{1}{2}\frac{c_3^2\left(d_3^2-d_1^2\right)}{c_1^2d_1^2-c_3^2d_2^2}\left[w_x\left(\begin{matrix}x+h,\\ L-\dfrac{h}{2}\end{matrix}\begin{matrix}\dfrac{h}{2}\\ ,t\end{matrix}\right)-w_x\left(\begin{matrix}x-h,\\ L-\dfrac{h}{2}\end{matrix}\begin{matrix}\dfrac{h}{2}\\ ,t\end{matrix}\right)\right], \tag{A.4c}$$

$$w_y\left(\begin{matrix}x,\\ L+\dfrac{h}{2}\end{matrix}\begin{matrix}-\dfrac{h}{2}\\ ,t\end{matrix}\right)=w_y\left(\begin{matrix}x,\\ L-\dfrac{h}{2}\end{matrix}\begin{matrix}\dfrac{h}{2}\\ ,t\end{matrix}\right)$$

$$\pm\frac{d_2^2\left(c_1^2-c_2^2\right)}{c_1^2d_1^2-c_3^2d_2^2}\left[u_x\left(\begin{matrix}x+h,\\ L-\dfrac{h}{2}\end{matrix}\begin{matrix}\dfrac{h}{2}\\ ,t\end{matrix}\right)-u_x\left(\begin{matrix}x-h,\\ L-\dfrac{h}{2}\end{matrix}\begin{matrix}\dfrac{h}{2}\\ ,t\end{matrix}\right)\right]$$

$$\pm\frac{1}{2}\frac{c_1^2d_3^2-c_3^2d_2^2}{c_1^2d_1^2-c_3^2d_2^2}\left[w_x\left(\begin{matrix}x+h,\\ L-\dfrac{h}{2}\end{matrix}\begin{matrix}\dfrac{h}{2}\\ ,t\end{matrix}\right)-w_x\left(\begin{matrix}x-h,\\ L-\dfrac{h}{2}\end{matrix}\begin{matrix}\dfrac{h}{2}\\ ,t\end{matrix}\right)\right], \tag{A.4d}$$

in which, (A.4c) and (A.4d) related to $y = -h/2$ is valid only along the crack surface, namely, only for $x \le a - h/2$ at $y = 0$, in which the crack terminates. From the last condition of (2.5), at $y = 0$ and the ahead of the crack, $u_y = 0,\ w_y = 0$. To satisfy this condition the displacements u_y and w_y at $y = -h/2$ are approximated by

$$\begin{aligned} u_y\left(x, -\frac{h}{2}, t\right) &= -u_y\left(x, \frac{h}{2}, t\right), \\ w_y\left(x, -\frac{h}{2}, t\right) &= -w_y\left(x, \frac{h}{2}, t\right). \end{aligned} \tag{A.5}$$

In constructing the approximation ((A.2a)-(A.2b)–(A.5)) we follow a method proposed by Alterman and Rotenberg. According to this method, derivatives perpendicular to the boundary are proposed by uncentered differences and derivatives parallel to the boundary by centered difference. The real boundary can be considered as located at a distance of half the mesh size from the grid boundaries. The four grid corners require a special treatment. Difference methods of handling the discontinuities at such points have been proposed in the past. Here we found that satisfactory results are obtained when the displacements sought are extrapolated from those given along both sides of the corner in question. Accordingly, the components u_x, u_y, w_x, w_y at $(-h/2, -h/2)$ are given by

$$\begin{aligned} \begin{matrix} u_x \\ u_y \end{matrix}\left(\frac{-h}{2}, -\frac{h}{2}, t\right) &= \begin{matrix} u_x \\ u_y \end{matrix}\left(\frac{h}{2}, \frac{-h}{2}, t\right) + \begin{matrix} u_x \\ u_y \end{matrix}\left(\frac{-h}{2}, \frac{h}{2}, t\right) \\ &\quad - 0.5\left[\begin{matrix} u_x \\ u_y \end{matrix}\left(\frac{3h}{2}, \frac{-h}{2}, t\right) \begin{matrix} u_x \\ u_y \end{matrix}\left(\frac{-h}{2}, \frac{3h}{2}, t\right)\right], \\ \begin{matrix} w_x \\ w_y \end{matrix}\left(\frac{-h}{2}, \frac{-h}{2}, t\right) &= \begin{matrix} w_x \\ w_y \end{matrix}\left(\frac{h}{2}, \frac{-h}{2}, t\right) + \begin{matrix} w_x \\ w_y \end{matrix}\left(\frac{-h}{2}, \frac{h}{2}, t\right) \\ &\quad - 0.5\left[\begin{matrix} w_x \\ w_y \end{matrix}\left(\frac{3h}{2}, \frac{-h}{2}, t\right) + \begin{matrix} w_x \\ w_y \end{matrix}\left(\frac{-h}{2}, \frac{3h}{2}, t\right)\right]. \end{aligned} \tag{A.6}$$

Similar expressions are used for deriving the displacement components at $(-h/2, H + h/2)$, $(L + h/2,\ L + h/2)$, and $(L + h/2, -h/2)$. By following relevant stability criterion of the scheme, the computation is always stable and achieves high exactness. The detailed introduction can be seen in [2].

Acknowledgments

The authors are very grateful to the reviewers for their helpful suggestions and patient assistance. The work is supported by the National Natural Science Foundation of China (Grant no. 10672022 and 10972035).

References

[1] D. Shechtman, I. Blech, D. Gratias, and J. W. Cahn, "Metallic phase with long-range orientational order and no translational symmetry," *Physical Review Letters*, vol. 53, no. 20, pp. 1951–1953, 1984.

[2] T. Y. Fan, *Mathematical Theory of Elasticity of Quasicrystals and Its Applications*, Science Press, Beijing, China; Springer, Heideberg, Germany, 2010.
[3] P. Bak, "Phenomenological theory of icosahedral incommensurate ("Quasiperiodic") order in Mn-Al alloys," *Physical Review Letters*, vol. 54, pp. 1517–1519, 1985.
[4] D. H. Ding, W. Yang, C. Hu, and R. Wang, "Generalized elasticity theory of quasicrystals," *Physical Review B*, vol. 48, no. 10, pp. 7003–7010, 1993.
[5] N. Inoue, "Dental problems in puberty," *Shikai tenbo = Dental outlook*, vol. 65, no. 7, pp. 1517–1522, 1985.
[6] P. Bak, "Symmetry, stability, and elastic properties of icosahedral incommensurate crystals," *Physical Review B*, vol. 32, no. 9, pp. 5764–5772, 1985.
[7] T. C. Lubensky, S. Ramaswamy, and J. Toner, "Hydrodynamics of icosahedral quasicrystals," *Physical Review B*, vol. 32, no. 11, pp. 7444–7452, 1985.
[8] A. Y. Zhu and T. Y. Fan, "Dynamic crack propagation in decagonal Al-Ni-Co quasicrystal," *Journal of Physics Condensed Matter*, vol. 20, no. 29, Article ID 295217, 2008.
[9] X. F. Wang, T. Y. Fan, and A. Y. Zhu, "Dynamic behaviour of the icosahedral Al-Pd-Mn quasicrystal with a Griffith crack," *Chinese Physics B*, vol. 18, no. 2, pp. 709–714, 2009.
[10] J. Wang, L. Mancini, R. Wang, and J. Gastaldi, "Phonon- and phason-type spherical inclusions in icosahedral quasicrystals," *Journal of Physics Condensed Matter*, vol. 15, no. 24, pp. L363–L370, 2003.
[11] J. Wang, W. Yang, and R. Wang, "Atomic model of anti-phase boundaries in a face-centred icosahedral Zn-Mg-Dy quasicrystal," *Journal of Physics Condensed Matter*, vol. 15, no. 10, pp. 1599–1611, 2003.
[12] D. Caillard, F. Mompiou, L. Bresson, and D. Gratias, "Dislocation climb in icosahedral quasicrystals," *Scripta Materialia*, vol. 49, no. 1, pp. 11–17, 2003.
[13] M. Feuerbacher, M. Bartsch, B. Grushko, U. Messerschmidt, and K. Urban, "Plastic deformation of decagonal Al-Ni-Co quasicrystals," *Philosophical Magazine Letters*, vol. 76, no. 6, pp. 369–375, 1997.
[14] D. Caillard, G. Vanderschaeve, L. Bresson, and D. Gratias, "Transmission electron microscopy study of dislocations and extended defects in as-grown icosahedral Al-Pd-Mn single grains," *Philosophical Magazine A*, vol. 80, no. 1, pp. 237–253, 2000.
[15] U. Messerschmidt, M. Bartsch, M. Feuerbacher, B. Geyer, and K. Urban, "Friction mechanism of dislocation motion in icosahedral Al-Pd-Mn quasicrystals," *Philosophical Magazine A*, vol. 79, no. 9, pp. 2123–2135, 1999.
[16] T. Y. Fan, "A study on the specific heat of a one-dimensional hexagonal quasicrystal," *Journal of Physics Condensed Matter*, vol. 11, no. 45, pp. L513–L517, 1999.
[17] T. Y. Fan, X. F. Li, and Y. F. Sun, "A moving screw dislocation in a one-dimensional hexagonal quasicrystal," *Acta Physica Sinica*, vol. 8, no. 4, pp. 288–295, 1999.
[18] T. Y. Fan and Y. W. Mai, "The partition function and state equation of the point group 12mm two-dimensional dodecagonal quasicrystal," *European Physical Journal B*, vol. 31, no. 1, pp. 25–27, 2003.
[19] C. L. Li and Y. Y. Liu, "Phason-strain influence on low-temperature specific heat of the decagonal Al-Ni-Co quasicrystal," *Chinese Physics Letters*, vol. 18, no. 4, p. 570, 2001.
[20] C. Li and Y. Liu, "Low-temperature lattice excitation of icosahedral Al-Mn-Pd quasicrystals," *Physical Review B*, vol. 63, no. 6, Article ID 064203, pp. 642031–642038, 2001.
[21] S. B. Rochal and V. L. Lorman, "Anisotropy of acoustic-phonon properties of an icosahedral quasicrystal at high temperature due to phonon-phason coupling," *Physical Review B*, vol. 62, no. 2, pp. 874–879, 2000.
[22] M. Shmuely and Z. S. Alterman, "Crack propagation analysis by finite differences," *Journal of Applied Mechanics*, vol. 40, no. 4, pp. 902–908, 1973.
[23] T. Y. Fan, X. F. Wang, W. Li, and A. Y. Zhu, "Elasto-hydrodynamics of quasicrystals," *Philosophical Magazine*, vol. 89, no. 6, pp. 501–512, 2009.
[24] K. Edagawa and Y. G. So, "Experimental evaluation of phonon-phason coupling in icosahedral quasicrystals," *Philosophical Magazine*, vol. 87, no. 1, pp. 77–95, 2007.
[25] S. B. Rochal and V. L. Lorman, "Minimal model of the phonon-phason dynamics in icosahedral quasicrystals and its application to the problem of internal friction in the i-AlPdMn alloy," *Physical Review B*, vol. 66, no. 14, Article ID 144204, pp. 1442041–1442049, 2002.
[26] K. Edagawa and S. Takeuchi, *Chapter 76, Dislocation in Solid*, Edited by F. R. N. Nabarro and J. P. Hirth, 2007.
[27] H. C. Jeong and P. J. Steinhardt, "Finite-temperature elasticity phase transition in decagonal quasicrystals," *Physical Review B*, vol. 48, no. 13, pp. 9394–9403, 1993.
[28] D. H. Ding, W. Yang, C. Hu, and R. Wang, "Generalized elasticity theory of quasicrystals," *Physical Review B*, vol. 48, no. 10, pp. 7003–7010, 1993.

[29] D. H. Ding, W. G . Yang, C. Z. Hu, and R. H. Wang, "Linear elasticity theory of quasicrystals and defects in quasicrystals," *Materials Science Forum*, vol. 150-151, pp. 345–354, 1994.
[30] W. Yang, R. Wang, D. H. Ding, and C. Hu, "Linear elasticity theory of cubic quasicrystals," *Physical Review B*, vol. 48, no. 10, pp. 6999–7002, 1993.
[31] C. Walz, *Zur Hydrodynamik in Quasikristallen*, Diplomarbeit, Universitaet Stuttgart , 2003.
[32] R. Mikulla, J. Stadler, F. Krul, H. R. Trebin, and P. Gumbsch, "Crack propagation in quasicrystals," *Physical Review Letters*, vol. 81, no. 15, pp. 3163–3166, 1998.
[33] P. Ebert, M. Feuerbacher, N. Tamura, M. Wollgarten, and K. Urban, "Evidence for a cluster-based structure of AlPdMn single quasicrystals," *Physical Review Letters*, vol. 77, no. 18, pp. 3827–3830, 1996.